RAPID COMMUNICATIONS

PHYSICAL REVIEW B VOLUME 47, NUMBER 3 15 JANUARY 1993-I

Atomic structure and doping of microtubules

Jae-Yel Yi and J. Bernholc
Department of Physics, North Carolina State University, Raleigh, North Carolina 27695-8202
(Received 8 June 1992)

The atomic and electronic structures of microtubules of graphitic carbon have been investigated by *ab initio* molecular dynamics. Fully optimized atomic structures of two microtubules, a reflection symmetric and a chiral, are found to differ little from their ideal, graphite-derived geometries. Both are semiconductors with direct band gaps at the Γ point and along the Δ direction, respectively. It is shown by direct calculations in large supercells that substitutional N and B dope microtubules *n* and *p* type.

Very recently, a new form of carbon clusters was discovered by high-resolution transmission electron microscopy[1] and identified as graphitic microtubules with diameters of a few nanometers. These microtubules, consisting of a cylindrical network of hexagonal rings, were found near the negative carbon electrode in the Krätschmer-Huffman apparatus.[2] Previous theoretical studies have shown that a microtubule is either metallic or semiconducting depending on its diameter and chirality.[3–5] The presence of semiconducting and metallic one-dimensional structures in the same family of materials opens up exciting possibilities of new phenomena and novel device structures.

Previous studies of the electronic structure of microtubules were carried out using either the ideal tubule geometry[3,5] or the one optimized with the help of a classical potential.[4] In this paper, we report the results of large-scale *ab initio* molecular-dynamics calculations for two tubule structures, one possessing reflection symmetry and the other chiral. The atomic structures of these tubules are fully optimized by *ab initio* forces and their band structures are determined in the local-density approximation. Both tubules are semiconductors with direct band gaps. Since carbon atoms are only threefold coordinated in the tubules, shallow doping of microtubules with group-V and group-III elements cannot be taken for granted. We tested the possibility of doping and found that substitutional nitrogen and boron are shallow donors and acceptors, respectively.

The *ab initio* molecular-dynamics (Car-Parrinello) method[6] iteratively solves the local-density equations using plane waves and the pseudopotential formalism.[7] In order to reduce the computational time, soft-core pseudopotentials were generated by moving the cutoff radii of the pseudopotentials slightly outwards. The carbon pseudopotential was previously shown to reproduce well the structural properties of diamond,[8] graphite, and solid C_{60}.[9] The N and B pseudopotentials were previously employed in a study of impurities in diamond. We used plane waves with kinetic energies smaller than 26 Ry for all the calculations except those involving nitrogen, where a 35-Ry cutoff was used. The exchange and correlation contributions to the total energy were calculated using the parametrized Ceperley-Alder exchange-correlation potential.[10] The tubules were placed in large supercells, which led to a parallel array of tubules separated by 5 Å. This large distance was chosen to avoid interactions between the tubules.

We first describe the atomic and electronic structure of pure microtubules, using terminology introduced in Refs. 1 and 3–5. The reader may want to consult these references for additional discussion. One can construct numerous tubules by rolling the graphite sheet into a cylinder (see Fig. 1). Denoting a fixed lattice point in a graphite plane by *O*, a specification of another lattice point, *X*, which will fold onto *O* uniquely defines the tubule structure.[1,3–5] Alternatively, its structure can be defined by its diameter and chirality, or by the lattice vector *OX*. Due to the symmetry of the original graphite lattice, it is sufficient to consider the lattice vectors contained in the triangle outlined with heavy lines. We have chosen two relatively large tubules of similar diameter for the present study, *B*(1,0)10 and *B*(11,5) in the notation of Ref. 4. The points defining the corresponding lattice vectors are marked *A* and *B* in Fig. 1. Tubule *A* has reflection symmetry while tubule *B* is chiral. Their diameters are 7.88 and 7.54 Å and their unit cells contain 40 and 22 atoms, respectively. In order to simplify the process of geometry optimization, we chose to perform structural relaxations in cells containing 80 and 88 atoms for tubules *A* and *B*, respectively. The cells are sufficiently large to use only Γ point sampling in the integration of the charge density over the Brillouin zone. The length of each supercell along the tubule axis was fixed by using the graphite bond length (1.42 Å) and the ideal tubule geometry. All the internal coordinates of the

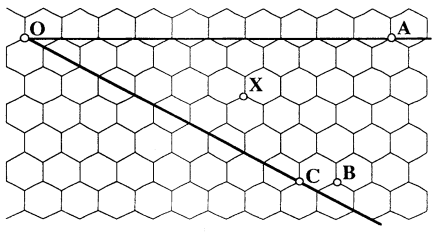

FIG. 1. Atomic structure of microtubules. Tubules *A* and *B* are constructed by rolling the graphite sheet into cylinders with points *A* and *B*, respectively, folding onto point *O*. The tubule generated by folding point *C* onto *O* is metallic. See the text.

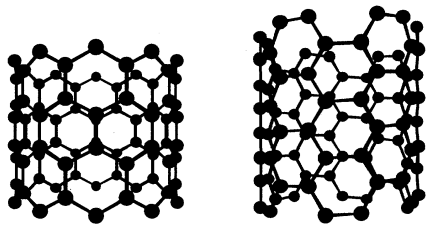

(a) (b)

FIG. 2. The relaxed atomic structures of tubules A (a) and B (b).

atoms in the supercells were relaxed using *ab initio* forces. Imposing periodic boundary conditions on the chiral tube B leads to a stress and results in slight splittings of the carbon-carbon bond lengths (see below).

The optimized structure of tubule A is shown in Fig. 2(a). The changes from the ideal tubule geometry are very small, although two kinds of bond lengths exist, 1.42 and 1.43 Å, due to the fixed length of the supercell. The deviations from its average radius of 3.98 Å are less than 0.01 Å. These variations are too small to significantly affect the band structure of the tubule. Figure 2(b) shows the optimized atomic structure of tubule B. The periodicity constraint on the unit cell of this tubule leads to three bond lengths, 1.41, 1.43, and 1.44 Å, but the changes from the ideal geometry are again small. The deviations from the average radius of 3.77 Å do not exceed 0.01 Å. Clearly, these results support the assumptions of Refs. 3–5, that the curvature of the tubules leads only to small distortions from the ideal geometries. The graphitic bonding character is preserved in the tubules, although their curvature allows for a partial mixing of σ and π states.

Band-structure calculations for systems as large as tubules A and B can be very expensive. A method that we call a "k-trajectory calculation" was used to reduce their cost. In this method, the eigenvalues $\varepsilon(\mathbf{k})$ are computed by varying $\mathbf{k}$ continuously along a given path. The wave functions at the next $\mathbf{k}$ point are obtained from those of the previous $\mathbf{k}$ point, resulting in fast convergence and excellent accuracy. For the band-structure calculations, the primitive unit cells consisting of 40 and 22 atoms for tubules A and B, respectively, were used.

The band structure of tubule A [$B(1,0)10$ in the notation of Hamada, Sawada, and Oshiyama] is shown in Fig. 3(a). As pointed out by earlier workers,[4,5] the band structures of tubules can be qualitatively explained using earlier results for single graphite sheets.[11] In the hexagonal Brillouin zone of the graphitic sheet the valence and conduction bands are degenerate at the K point (see Fig. 4) leading to the well-known semimetallic behavior of graphite. At all other points a gap separates the bonding and the antibonding states. In a tubule, the requirement of continuity of the wave functions upon a rotation by 2π around the axis of the tubule allows only for discrete values of k vectors parallel to its circumference. This leads to evenly spaced lines of allowed k vectors.[4] In Fig.

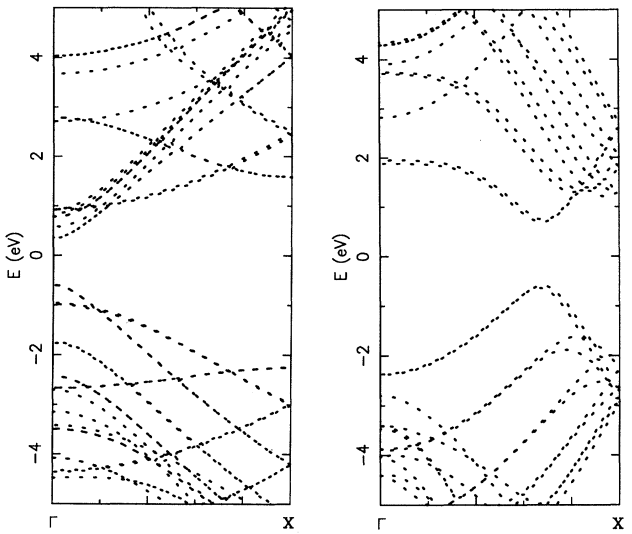

(a) (b)

FIG. 3. The band structures of tubules A (a) and B (b) in their respective Brillouin zones. See the text.

4(a) we show the projection of allowed k vectors onto the Brillouin zone of graphite for tubule A. The K points of the graphite sheet are not allowed, leading to a band gap. The band gap occurs at the Γ point, is direct, and has a value of 0.96 eV.

The band structure of tubule B [$B(11,5)$ in the notation of Hamada, Sawada, and Oshiyama] is shown in Fig. 3(b). The band gap occurs along Δ around $\frac{2}{3}X$, is direct, and has a value of 1.28 eV. The position of the gap can be explained by referring to the band structure of graphite and that of metallic tubules of the form $B(2,1)n$.

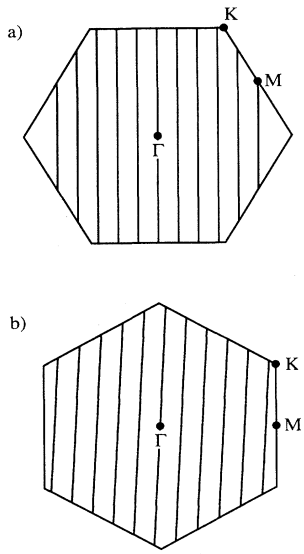

FIG. 4. The lines of allowed k points in the hexagonal Brillouin zone of a graphite sheet for (a) tubule A and (b) tubule B. See the text.

Reference 4 has shown that in the tubules of this form the lines of allowed k points are perpendicular to the ΓM line and divide it into n equally spaced segments. In particular, points along the KM line are allowed. The K point of the graphite sheet translates to $\frac{2}{3}X$ in the $B(2,1)n$ tubules, resulting in band crossing at $\frac{2}{3}X$ in the tubules. Although the $B(11,5)$ tubule is chiral and is studied for the first time in the present paper, a similar analysis is still applicable. For $B(11,5)$ the lines of allowed k points are spaced by $\frac{2}{11}$ of the ΓM distance; see Fig. 4(b). Due to the chirality, they are no longer perpendicular to ΓM. Since K is not an allowed k point, tubule B is a semiconductor, with the band gap still occurring near $\frac{2}{3}X$. The gap is direct, since near K the highest occupied and the lowest unoccupied graphite bands are symmetric about the Fermi level. By comparing Figs. 4(a) and 4(b) one can notice that the allowed k points of tubule B are somewhat further away from K than those of A, which results in a greater band gap of tubule B. One should point out that the calculated band gaps of both tubules are likely to be significantly underestimated, since they were computed using the local-density theory.

The band gap of tubule A has been previously computed using the semiempirical tight-binding method.[4] The local-density band gap is larger by 0.1 eV than that quoted in Ref. 4. The chiral tubule B has been considered for the first time in the present paper, but a nearby metallic $B(2,1)6$ tubule has been studied in Ref. 4. A detailed comparison to the tight-binding results of Ref. 4 is difficult, however, because the band structures plotted in this reference are for tubules with different diameters and chiralities. Nevertheless, it is clear that the two sets of results are qualitatively similar and that the agreement is substantially better for the valence bands than for the conduction bands. This is due to the well-known difficulties of the empirical tight-binding method in describing the dispersion of conduction bands in semiconductors. In Ref. 3 the metallic tubule $B(2,1)5$ has been studied in the local-density approximation. Due to structural similarities between this tubule and tubule B, their band structures are similar, although the latter is a semiconductor.

We now turn to the doping of tubules. Tubule A was chosen as a paradigmatic case and we consider substitutional N and B. The calculations were carried out in the 80-atom unit cell and the geometry was fully optimized by *ab initio* forces. We first describe the N-doped tubule. After substitution of one of the C atoms with N, atomic relaxation results in a total energy gain of 0.25 eV, but changes from the original atomic positions around the N impurity are less than 0.02 Å. The impurity level induced by N is located 0.27 eV below the bottom of the conduction band in our supercell.[12] The contour plot of its charge density along the surface of the tubule is shown in Fig. 5(a). The plot shows that the N wave function is quite extended and overlaps significantly with that of the adjacent N atom. Further analysis reveals that its orbital content is mainly π and that this wave function is derived mainly from the conduction bands of the pure tubule.

In the case of boron, the relaxation energy is 0.63 eV and the local atomic distortions are larger. The B atom

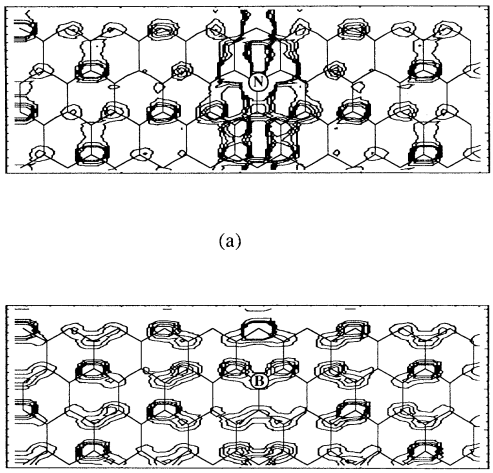

FIG. 5. Contour plots of charge densities of the impurity levels introduced by (a) N doping and (b) B doping. The plotting plane is along the surface of the tubule. See the text.

and its nearest-neighbor C atoms move outwards by up to 0.11 Å and the average C-B bond length becomes 1.49 Å. The greater distortion is due to the larger covalent radius of B. However, the C-C backbonds remain the original 1.42 Å. The calculated position of the B level in the 80-atom supercell is 0.16 eV above the top of the valence bands. The charge density associated with this level is even more delocalized than for N; see Fig. 5(b). A significant amount of charge occupies the C-C bonding regions. This is because the B wave function is mostly derived from the valence bands, as expected for an acceptor impurity.

Compared to doping in other carbon systems, N introduces a shallow level in the C_{60} molecule,[13] but is a deep donor in diamond.[14] In the C_{60} molecule, the N level is accidentally also 0.27 eV below the lowest unoccupied orbital.[13] The local relaxations and energy gains are also similar to those in the tubule. In diamond, however, N bonding is substantially different. When N is placed in the substitutional fourfold-coordinated site, it causes a distortion in which the N atom and one of its neighbors move away from each other, leading to a 25% increase in their separation and a total energy gain of 0.76 eV.[8] This configuration leads to a doubly occupied N lone pair and a C dangling bond 1.6 eV below the bottom of the conduction band of diamond.

Boron is a well-known substitutional shallow acceptor in diamond with an energy level 0.37 eV above the top of the valence bands.[15] In the C_{60} molecule, its level was calculated to be 0.45 eV above the highest occupied molecular orbital.[13] Although the extent of the B-induced wave function is ultimately limited by the size of the isolated C_{60} cluster, the B wave function is localized around B and its close neighbors. The B relaxation energy is greater in C_{60} than in the tubule (1.2 vs 0.63 eV) and the atomic relaxations are correspondingly larger. Al-

though B doping of C_{60} molecules has already been achieved,[16] the position of the B level has not yet been determined.

In summary, we have investigated the atomic and electronic structure of paradigmatic pure and doped microtubules of graphitic carbon. The optimized geometry of the tubules retains well the characteristics of graphite. The deviations from the ideal structures are small. It is possible to fabricate microtubules with direct band gaps away from the Γ point by exploiting the similarities between the projected band structure of graphite and that of the tubule. The semiconducting tubules can be doped *n* and *p* type by substitutional N and B, respectively. It is thus possible to make one-dimensional doped structures with novel physical and device characteristics.

This work was supported by ONR, Grant No. N00014-91-J-1516. The supercomputer calculations were carried out at the NC Supercomputing Center.

[1]S. Iijima, Nature **354**, 56 (1991).
[2]W. Krätschmer, L. D. Lamb, K. Fostiropoulos, and D. R. Huffman, Nature (London) **347**, 354 (1990).
[3]J. W. Mintmire, B. I. Dunlap, and C. T. White, Phys. Rev. Lett. **68**, 631 (1992).
[4]N. Hamada, S.-I. Sawada, and A. Oshiyama, Phys. Rev. Lett. **68**, 1579 (1992).
[5]R. Saito, M. Fujita, G. Dresselhaus, and M. S. Dresselhaus, Appl. Phys. Lett. **60**, 2204 (1992).
[6]R. Car and M. Parrinello, Phys. Rev. Lett. **55**, 2471 (1985).
[7]D. R. Hamann, M. Schluter, and C. Chiang, Phys. Rev. Lett. **43**, 1494 (1979); D. R. Hamann, Phys. Rev. B **40**, 2980 (1990).
[8]S. A. Kajihara, A. Antonelli, and J. Bernholc, Phys. Rev. Lett. **66**, 2010 (1991).
[9]Q.-M. Zhang, J.-Y. Yi, and J. Bernholc, Phys. Rev. Lett. **66**, 2633 (1991).
[10]D. M. Ceperley and B. J. Alder, Phys. Rev. Lett. **45**, 566 (1980); J. Perdew and A. Zunger, Phys. Rev. B **23**, 5048 (1981).
[11]J. C. Slonczewski and P. R. Weiss, Phys. Rev. **109**, 272 (1958).
[12]The level positions are given at the Γ point. Due to the extended nature of the shallow levels' wave functions, some broadening of the impurity levels is to be expected in supercell calculations. The computation of this broadening is prohibitively expensive at present.
[13]W. Andreoni, F. Gygi, and M. Parrinello, Chem. Phys. Lett. **190**, 159 (1992).
[14]R. G. Farrer, Solid State Commun. **7**, 685 (1969).
[15]A. W. S. Williams, E. C. Lightowlers, and A. T. Collins, J. Phys. C **3**, 1727 (1970); J. C. Bourgoin, J. Krynicki, and B. Blanchard, Phys. Status Solidi A **52**, 293 (1979).
[16]T. Guo, C. Jin, and R. E. Smalley, J. Phys. Chem. **95**, 4948 (1991).